MDPI

Article

Ciprofloxacin Removal Using Pillared Clays

Lourdes Jara-Cobos [1], María Eulalia Peñafiel [1], Carolina Montero [2], Miguel Menendez [3] and Veronica Pinos-Vélez [1,4,*]

1 Grupo de Ingeniería de las Reacciones Químicas, Catálisis y Tecnologías del Medio Ambiente (IRCMA), Departamento de Biociencias, Universidad de Cuenca, Ecocampus Balzay, Cuenca 010202, Ecuador; lourdes.jara@ucuenca.edu.ec (L.J.-C.)
2 Facultad de Ingeniería Química, Universidad Central del Ecuador, Ritter s/n y Bolivia, Quito 170129, Ecuador
3 Catalysis, Molecular Sparations and Reactor Engineering Group (CREG), Aragon Institute of Engineering Research (I3A), Universidad Zaragoza, 50018 Zaragoza, Spain
4 Departamento de Recursos Hídricos y Ciencias Ambientales, Universidad de Cuenca, Eco-Campus Balzay, Av. Víctor Manuel Albornoz, Cuenca 010202, Ecuador
* Correspondence: veronica.pinos@ucuenca.edu.ec

Abstract: In this work, Ti-pillared bentonites were evaluated to remove ciprofloxacin (CIP) from the aqueous solution. Pillared sodium bentonite (BSP) and pillared calcium bentonite (BCP) were prepared by means of the sol–gel method using titanium tetraisopropoxide with calcination for 3 h at 500 °C. They were characterized using the BET method for N_2 adsorption, and subjected to X-ray diffraction and Fourier transform infrared spectroscopy. The results show that the surface area of the pillared bentonites increased after the process, more than the natural ones. Pillared sodium bentonite has a more porous structure, larger surface areas, and higher adsorption capacity than pillared calcium bentonite. The kinetic adsorption of ciprofloxacin (CIP) onto pillared bentonites is well described by the pseudo second-order kinetic model. The BSP isotherm well fitted the Freundlich model, while the BCP isotherm fits the BET model better, suggesting multilayer adsorption. DR model shows mostly physical adsorption for CIP on the two adsorbents. The pH influence study indicated that CIP is adsorbed at pH between 6 and 8, which facilitates the use of BCP and BSP in wastewater treatment, whose pH generally oscillates between these ranges.

Keywords: clay; pillared; removal; ciprofloxacin; bentonite

1. Introduction

Ciprofloxacin (CIP) is a broad-spectrum antibacterial agent used in the treatment of a wide variety of infections, principally those caused by Gram-negative pathogens, such as tract infections, sexually transmitted diseases, skin and bone infections, gastrointestinal infections, lower respiratory tract infections, febrile neutropenia, intra-abdominal infections, and malignant external Otitis [1,2]. CIP ($C_{17}H_{18}FN_3O_3$) is a new generation of fluorinated quinolones structurally related to nalidixic acid [3,4]. CIP is available in intravenous and oral formulations; it has an approximate bioavailability of 70–80% after oral administration and is concentrated in various body tissues and fluids. CIP is fundamentally excreted unmetabolized in the urine (40% to 50%) and feces (20% to 35%) in approximately 3 or 5 h [1,3]. Additionally, small amounts of metabolites have been found to be oxo ciprofloxacin, sulociprofloxacin, diethylene ciprofloxacin, and formyl ciprofloxacin; these four metabolites account for 15% of a total oral dose [5].

Due to its many advantages, despite being a medication that requires a prescription, CIP is one of the most widely used antibiotics worldwide [6]. Oral treatment lasts one to two weeks and is administered twice daily [3]. It is used in both humans and animals, and at times CIP is also found in the milk and meat of animals sold for human consumption [7,8]. As mentioned above, much of this compound is excreted in urine and feces, thus ending up in wastewater [9,10]. Considering that it presents a high solubility of approximately

30 gL^{-1} at 20 °C [5], facilitating their mobility in the water, it is not surprising that CIP is part of the so-called emerging contaminants in water. CIP was found in the surface water of 20 countries worldwide, with an average concentration of 19 µgL^{-1} [7]. For instance, CIP was found in 90% of the samples with an average concentration of 93.3 µgL^{-1} in the Bosten Lake located in Xinjiang system [11].

This is a matter of grave concern because the occurrence of antibiotics in low concentrations in waters is associated with bacterial resistance [12]. For this reason, ciprofloxacin must be considered in water treatments. However, due to its complex chemical structure, conventional treatments cannot remove it [13], and its presence in the aquatic environment could portend serious toxicity for aquatic flora and fauna species [14]. Many technologies, including microbial degradation and chemical and physical treatment, have been developed to remove antibiotics from wastewater [4,9,15]. There is a wide variety of expensive technologies, such as reverse osmosis, membrane separation, chemical precipitation, advanced oxidation, and ion exchange, however, one of the most promising methods is adsorption, particular due to its low cost [15,16].

Various types of biomass and polymeric adsorbents have been tried which have shown good results [17–23]. Among these, clays have shown promising results in the adsorption of antibiotics, mainly CIP; composites of clays and clay minerals have gained considerable attention in recent years due to their increased adsorption capacity, ease of recovery from aqueous solutions, and improved physicochemical properties [22]. Bentonites stand out for their high adsorption capacity, easy availability, and low-cost [16]. It is a widely distributed clay material resulting from the devitrification and chemical alteration of glassy volcanic ash or tuff. Bentonite is composed predominantly of smectite minerals, principally montmorillonite. Its characteristic minerals are crystalline with a micaceous habit, high birefringence, and facile cleavage. It has high adsorptive powers; this property is more dependent on its physical form, i.e., the micaceous structure and easy cleavage which gives excellent surface area and texture and enables permeability, than its chemical composition. Analyses of the clay minerals from bentonite indicate that montmorillonite is the most widespread with the formula $(Mg, Ca)O\ Al_2O_3\ 5SiO_2, nH_2O$ [24]. Research has verified their ability to absorb antibiotics, such as CIP. For instance, some researchers used a natural bentonite to adsorb CIP successfully where the pseudo second-order kinetic model fitted adsorption kinetics for adsorbents. In this study, the thermodynamic of CIP adsorption shows that adsorption is endothermic adsorption and $\Delta G°$ for bentonite indicates the spontaneous nature of the adsorption [25]. Another research with bentonite to absorb CIP in batch experiments in different conditions found that the optimum contact time, pH, agitation speed, and adsorbent dosage were 30 min, 4.5 pH, 150 rpm, and 2.5 gL^{-1}, respectively. The isotherm adsorption data fitted well with the Langmuir model, and the data fitted well with the pseudo second-order kinetics [25]. However, its high affinity for water and relatively low specific surface area limits its use and subsequent separation from aqueous media. Several studies have shown that clay modifications, such as columnar formation, modify porosity by increasing clays' specific surface area and adsorption capacity.

Pillaring is a chemical process used to improve the adsorption capacity of clays, including bentonites. The objective of piling is to increase the interlaminar space between the clay layers, making a greater surface area available for the adsorption of molecules. Pillaring transforms a layered crystalline inorganic compound into a material with microporosity and mesoporosity [26]. To carry out the pillaring of bentonites, a pillaring agent is used, which is typically an inorganic compound that is inserted between the layers of clay. The pillaring agent replaces the cations in the bentonite structure, allowing a greater expansion of the clay layers, and therefore a greater adsorption capacity. Pillared InterLayered Clays (PILCs) are obtained from smectite clay minerals typically following this three-step synthesis procedure: (a) polymerization of a multivalent cation (Mg^{2+}, Al^{3+}, Cr^{3+}, and Fe^{3+}, among others), leading to polyhydroxocations; (b) intercalation of these polycations into the interlayer space of the clays, involving the substitution of natural

exchangeable charge-compensating cations; and (c) calcination at moderate temperatures which transforms the polycations into stable oxi-hydroxide phases named pillars. These pillars provide a more stable and resistant structure that increases the specific surface area and bentonite's porosity, improving its absorption capacity.

The adsorption capabilities of these materials make them an ideal alternative for treating water polluted with recalcitrant compounds, such as antibiotics [27]. For instance, low-cost and eco-friendly pillared clays with Al, Fe, Si, and Zr were tested under basic pH conditions to remove CIP in its anionic form (CIP-). The Si and Fe pillared clays achieved the highest adsorption capacities. The suggested adsorption mechanism involves forming inner-sphere complexes and van der Waals interactions between CIP- and the available adsorption sites on the surfaces of the pillared clay [28]. Another work used Fe and SiFe-pillared clays obtained from a mineral industry waste to successfully adsorb CIP in basic media [29]. Yet another study tested three silica pillared clays for CIP adsorption with a different pH, demonstrating that pH changes influence adsorption since the CIP changes its ionic form and gains or loses solubility [30]. However, most of the studies primarily used pillared clays as catalysts, but there are only a few studies focusing on their adsorbent capacities. A work with Ti- pillared clays increased the specific surface of clays, providing good results in the adsorption of several drugs [31]. Furthermore, Hamza et al. demonstrated that pillaring with Ti increased the specific surface area by a higher percentage than pillaring with Fe [32]. The pillars so formed are rigid and impart clay with enhanced and permanent porosity enabling it to serve as an effective adsorbent [33].
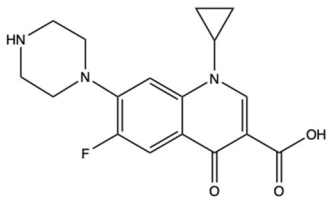
Taking the aforementioned observations into account, this present work aimed to pillarize two benthic clays, one sodium and the other calcium, using titanium oxide to improve their adsorption capacity in removing ciprofloxacin. The best conditions of pH, time, and dose were determined to obtain the maximum adsorption capacity of the CIP. In addition, the adsorption kinetics and the equilibrium of the process were determined.

2. Materials and Methods

2.1. Adsorbate

Ciprofloxacin (CAS: 85721-33-1), ≥98% HPLC grade, analytical grade supplied by Sigma Aldrich (Burlington, MA, USA), was used. Table 1 shows the ciprofloxacin properties.

Table 1. Ciprofloxacin structure and properties.

Molecular Structure †	
CAS	85721-33-1
Molecular weight	331.46 gmol^{-1}
Solubility in water *	30,000 mgL^{-1} at 20 °C
Acidic pKa *	6.16
Basic pKa *	8.62
log Kow *	0.28

Note: † ChemDraw 18; * PUBCHEM.

2.2. Adsorbents

The sodium and calcium clay were obtained from the ECUAMINERAL Company (Cuenca, Ecuador). The cation exchange capacity of clays is 202.55 meq 100 g^{-1} and 70.71 meq 100 g^{-1}, respectively.

Clays Pillarization

To perform the pillaring, Sigma Aldrich Ti[OCH(CH$_3$)$_2$]$_4$ titanium tetraisopropoxide and Sigma Aldrich Cl$_4$Ti titanium chloride were used. The pillaring agent was prepared using the sol–gel method, which was based on the dropwise addition of the reagents titanium tetraisopropoxide or titanium chloride in a 1 M HCl aqueous solution under continuous stirring for 3 h at 50 °C until obtaining a clean (clear) solution. The HCl/Ti molar ratio = 4 and the amount of titanium was 10 mmol per gram of montmorillonite. The titanium hydrate sol obtained is added dropwise to a suspension of montmorillonite in water (1% by weight) followed by stirring for 17 h and then proceeded to a sequence of washing with distilled water, centrifugation, and drying at 40 °C for 72 h. Finally, the modified clay was calcined at 500 °C for 3 h.

2.3. Adsorbents Characterization

The BET method determined the clay's surface area in a Micromeritics Autochem 2920 (Laboratorio de Investigación, Facultad de Ingeniería Química, Universidad Central del Ecuador). Before and after the adsorption process, the superficial chemical groups were analyzed using a PerkinElmer-Spectrum Two FTIR spectrometer with an ATR accessory.

The pH points of zero charges (pH_{pzc}) values of pillared adsorbents were determined using an equilibrium method in a batch system [17,23].

The determination of the components with defined crystallization present in the samples was carried out using a D2 PHASER Diffractometer, with the help of Difrac plus software for measurement, and EVA and TOPAS 4.2 for the identification and quantification of the crystalline phases present in each of the samples.

2.4. CPX Adsorption Investigations

Investigation of CIP adsorption on pillared bentonites was performed in a MaxQ4000 shaker at 20 °C. Initially, a stock solution of 20 mgL^{-1} CIP was prepared, from which 50 mL were taken and the tests were carried out, adding different weights of pillared sodium bentonite (BSP) and pillared calcium bentonite (BCP).

The pH effect was studied from 2 to 10 with an initial CIP solution concentration of 20 mgL^{-1}. The pH was adjusted with 0.1 N HCl and 0.1 N NaOH. The CIP adsorption kinetic was studied with the optimal dosage of each adsorbent varying the times between 5 and 90 min, and the concentration of CIP was 20 mgL^{-1}, and pH 6.5. Adsorption equilibrium data were collected in the concentration range of 5–60 mgL^{-1}. The solutions were filtered using Millipore 0.45 µm. All experiments were carried out in triplicate, and the average values were taken.

2.5. Removal Capacity

The initial and final CIP concentrations were determined using an ultraviolet-visible light spectrophotometer (UV-Vis), Thermo Scientific Genesys TM 10S (Waltham, MA, USA), by measuring at a maximum absorbance of 273 nm.

The amount of CIP adsorbed (q_e), and the following equations calculated the percent removal (%R) on pillared clays [34].

$$q_e = \frac{(Co - Ce)}{m} V \tag{1}$$

$$\%R = \frac{(Co - Ce)}{C_o} 100 \tag{2}$$

where, Co and Ce are the concentration of SMX in the initial solution and the aqueous phase after adsorption (mgL^{-1}), respectively; V is the volume of the solution (L); and m is the mass of the adsorbent (g).

The linear forms of pseudo first-order and pseudo second-order models were used to fit the kinetic data, while the linear forms of the Langmuir, Freundlich, BET, and Dubinin–Radushkevich equations modeled the adsorption isotherms, see Table 2.

**Table 2.** Models to fit the kinetic data and the linear forms.

Pseudo first order	$ln(q_e - q_t) = lnq_e - k_1 t$	[35]
Pseudo second order	$\frac{t}{q_t} = \frac{1}{k_2 q_e^2} + \frac{t}{q_e}$	[36]
Langmuir	$\frac{C_e}{q_e} = \frac{C_e}{q_m} + \frac{1}{k_L q_m}$	[37]
Freundlich	$logq_e = logk_F - \frac{1}{n}logC_e$	[37]
Brunauer–Emmett–Teller	$\frac{C_e}{q_e(C_s - C_e)} = \frac{1}{q_s C_{BET}} + \frac{(C_{BET}-1)C_e}{q_s C_{BET} C_s}$	[38]
Dubinin–Radushkevich isotherm	$lnq_e = lnq_s - k_{ad}eE^2$	[39]

Where, C_e is the concentration of CIP (mgL^{-1}); q_e is the equilibrum adsorption capacity and q_t the capacity adsorption at any time (mgg^{-1}); q_m is the maximum adsorption capacity (mgg^{-1}); k_L is the Langmuir (Lmg^{-1}); k_F is the Freundlich constant, (mgL^{-1}) $(mgg^{-1})^{-\frac{1}{n}}$; n refers to the adsorption intensity (dimensionless); q_S is the theoretical saturation capacity (mgg^{-1}); C_{BET} is the BET adsorption isotherm (Lmg^{-1}); C_S is adsorbate monolayer saturation concentration (mgL^{-1}); k_{ad} is a constant related to the mean free energy of adsorption (mg^2J^{-2}); and E is the polyani potential ($Jmol^{-1}$).

3. Result and Discussion

3.1. Characterization of Polarized Bentonites

The N_2 adsorption isotherms can be observed in Figure 1. The shape of the isotherms corresponds to type IV or a combination of type I and type II, which means that multilayer adsorption occurred on micro-mesoporous materials with an ordered chemical structure. The hysteresis of both materials is of the H_4 type typical of mesoporous materials. The higher amount of N_2 absorbed in BSP evidences a more porous structure in the BSP, which suggests that the pillaring process is better in BSP.
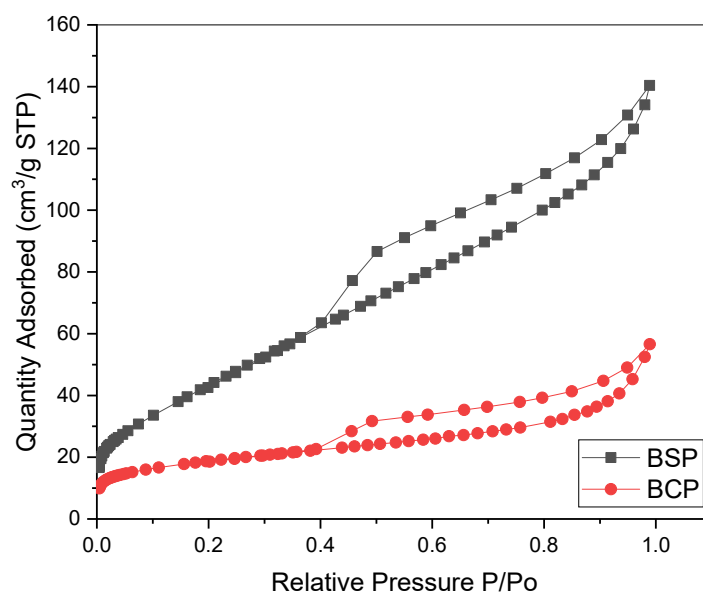
Figure 1. N_2 Adsorption–desorption isotherms of BSP and BCP.

The textural analysis of the pillared bentonites shows an increase in the surface areas with respect to natural bentonites. The surface area of natural calcium bentonite increased

from 42 m^2g^{-1} to 63 m^2g^{-1}, while sodium bentonite increased from 28 m^2g^{-1} to 162 m^2g^{-1} (Table 3). This increase in area is attributed to the increase in pores, as reported by Roca [30], who showed a greater surface area in columnar clays, which ultimately led to better adsorption, and the increase in surface area led to an increase in micropore volume. This may be due to the physicochemical transformations during the intercalation and calcination steps that are carried out to obtain BCP and BSP.

Table 3. Physical properties of pillared bentonites.

Clay	S_{BET} (m^2g^{-1})	Pore Volume (cm^3g^{-1})	Pore Size (nm)	Porosity (gcm^{-3})
BCP	63	0.08	3.5	2.2
BSP	162	0.21	3.0	2.2

The zero charge point pH values (pH_{pzc}) for BCP and BSP were equal to 4.2 and 4.1, respectively. This indicates that after the pillaring process, the clays are slightly more acidic than the natural ones whose pH_{pzc} has values of 7.80 and 9.85 for BCP and BSP, respectively, indicating that the integration of Ti increases the acidity of the clay.

Figure 2 shows the X-ray diffraction profile for BSP and BCP. The XRD pattern of BCP and BSP show a significant decrease in the degree of crystallinity after pillar formation, especially in BSP, which is due to the introduction of amorphous TiO_2 into the structure. The presence of well-defined peaks at positions 20°, 23° 27° and 50° in 2θ of the BCP spectrum shows a more crystalline structure than BSP. The amount of SiO_2 as quartz and elite is higher in BCP than in BSP [30,40]. These results explain the lower specific surface that BCP presents, as observed in Table 3.
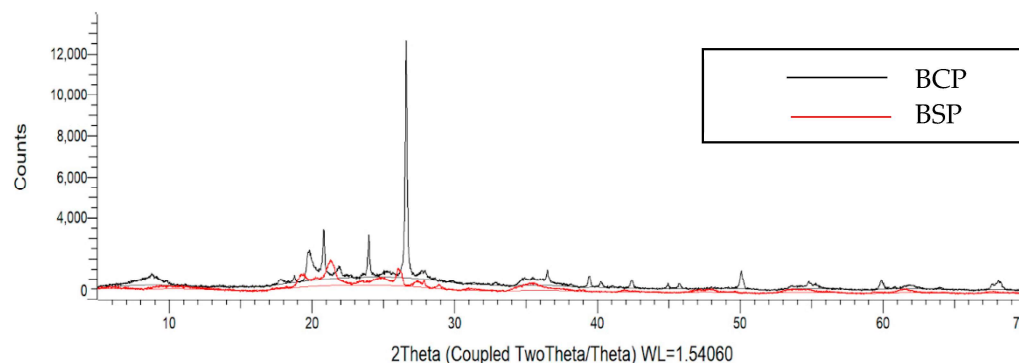
Figure 2. XRD patterns for pillared calcium bentonite and pillared sodium bentonite.

The results of the FTIR spectrum before and after adsorption are shown in Figure 3. FTIR provides information about functional groups present on the surface adsorbent. The BSP and BCP spectra show the Al-OH-Al bending bands at 918 cm^{-1} and the strongest band of Si stretch vibration is at –O–Si at 1029 cm^{-1} [28,41]. The out-of-plane vibrations of Al–O, and Si–O are shown at 650 cm^{-1}, while wavelengths between 500 and 800 can be attributed to the presence of quartz [41]. The distribution of the OH group between Fe and Al is observed between 700 and 900 cm^{-1}. After adsorption, new peaks appear, one in the 1350 cm^{-1} region that may correspond to the union of the CIP N-H group with the adsorbent and another in the 1620 cm^{-1} band that is attributed to the CIP carboxyl group [42,43].
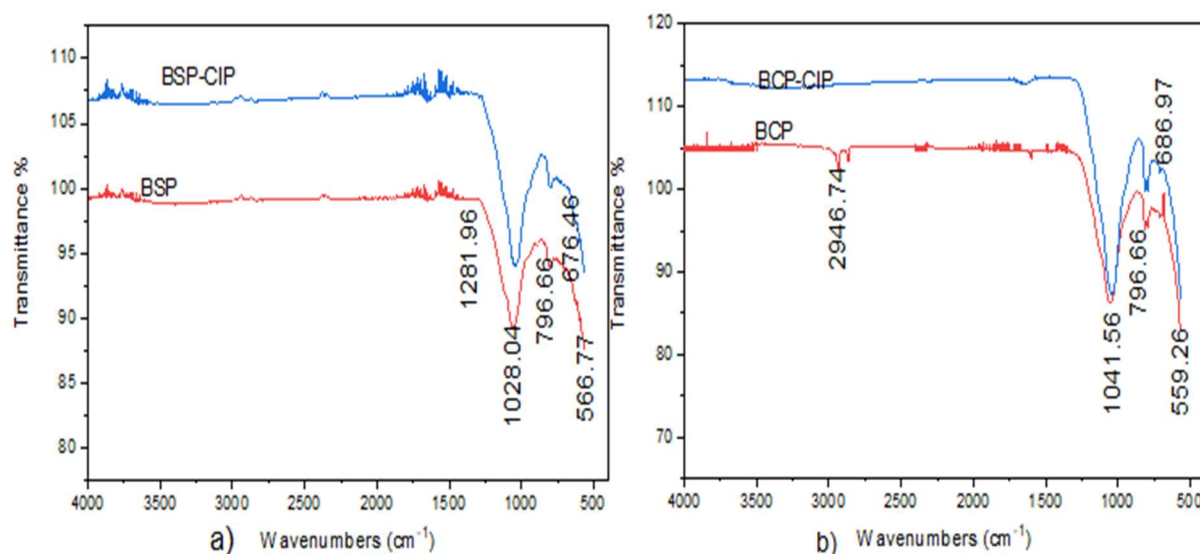
Figure 3. FTIR spectra (**a**) Pillarized sodium bentonite and sodium bentonite after CIP adsorption. (**b**) Pillarized calcium bentonite and calcium bentonite after CIP adsorption.

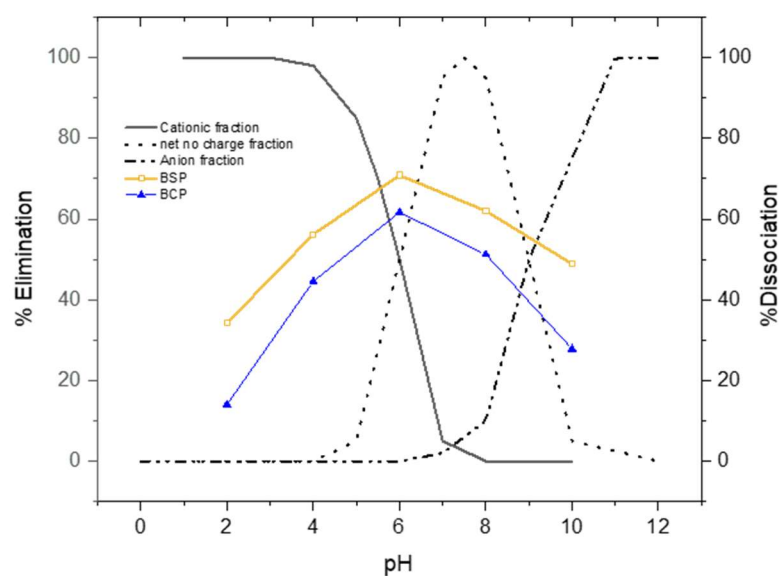### 3.2. Adsorption Studies

3.2.1. Effect of Bentonites Dosage

The amount of adsorbent to be used for the adsorption of a certain adsorbate is usually different for each material and depends on its physical and chemical characteristics. As observed in Table 3, there is a significant difference in the value of the surface area of BSP and BCP. BSP has a larger specific surface. A larger amount of adsorbent increases the number of active sites available for adsorption, so CIP removal percentages are high. However, a high amount of adsorbent decreases the adsorption capacity, because above a certain dose of adsorbent, a number of active sites remain unsaturated, and the percentage of removal does not increase. Therefore, the optimal amount of adsorbent must be found with which the highest percentage of removal is achieved without excessive adsorbent consumption.

Figure 4 shows the effect of the dose of each pillared bentonite on CIP adsorption. The optimal dose for both bentonites is 0.2 gL^{-1}, via which a removal of 62.7% (69 mgg^{-1}) is achieved with BCP and a removal of 70.5% (73.5 mgg^{-1}) is achieved with BSP. This dose is lower than that used (2.5 gL^{-1}) with other Al and Zr pillared clays [29,30,40,41].

The influence of the pH of the solution on the adsorption of CIP has been demonstrated in several studies [43,44]. They show that CIP is better adsorbed at pH between 6 and 8, a range in which the drug is dissociated, presenting both positive and negative charges. Figure 5 shows the influence of pH on CIP adsorption on pillared bentonites. It can be observed that the two bentonites present the same behavior with the variation of the pH, and it can be seen that the high amount of CIP adsorbed was obtained at a nearby pH of 6. At pH 6, pillared bentonites have a negative charge, while CIP has both positive and negative charges, aiding electrostatic attraction and increasing adsorption. At pH lower than pKa of 6.16 and values greater than pKa of 8.62, electrostatic repulsions between adsorbent and adsorbate hinder adsorption. The greater solubility of CIP at acidic pH also influences the decrease in adsorption at low pH. The higher adsorption at pH between 6 and 8 suggests that the adsorption is mainly due to the porosity of the material and the interactions with the active sites by Van der Walls forces due to electrostatic interactions. In the pH range of 6.0–8.7, the carboxylic group is deprotonated and negatively charged, while the amino group is protonated and positively charged. At a lower pH than 6 and a higher pH than 8, electrostatic repulsions decrease adsorption [45]. These results are helpful for removing CIP from wastewater, which generally has a pH between 6 and 8.
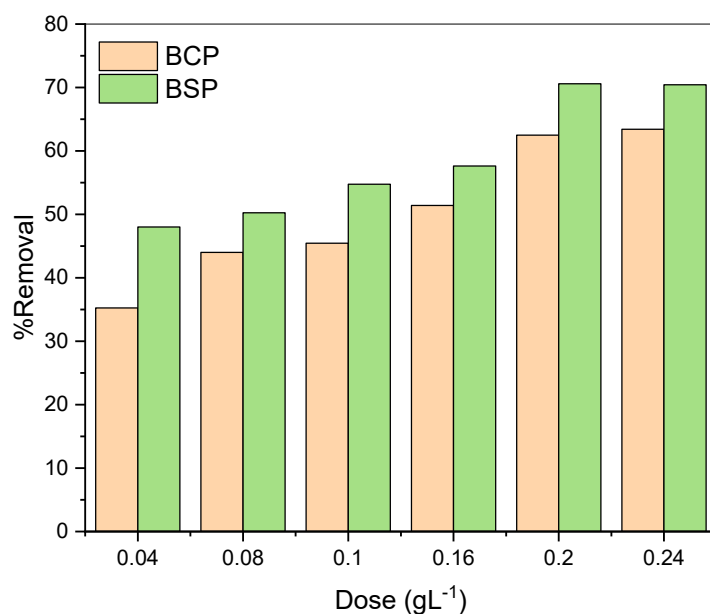
Figure 4. Doses of BSP and BCP according to the percentage of removal.

Figure 5. Influence of the pH of the solution on the adsorption of CIP at a Co = 20 mgL^{-1} with pillared calcium bentonite and pillared sodium bentonite.

3.2.2. Adsorption Kinetic

The kinetic studies for the two adsorbents were carried out at an initial concentration of 20 mgL^{-1} of CIP at pH 6.5. The adsorption increases considerably during the first 15 min; the time to reach equilibrium was 45 min for BCP and 60 min for BSP, the same was reported in other works [42,46]. These results showed rapid adsorption compared to other materials used in CIP removal [43]. The experimental data showed a better fit to the pseudo second-order model, which implies that the adsorption rate of BSP and BCP were mainly affected by the availability of active adsorption sites at the beginning of the process [47], similar to other works pertaining to CIP adsorption on various materials [42,44,46,48]. The data of the fits and the parameters of the pseudo first-order and pseudo second-order models are shown in Table 4 and Figure 6. The k_2 values for BCP are slightly higher than BSP, which can be associated with the shorter time required for BCP to reach equilibrium.

Table 4. Parameters of the pseudo first-order and pseudo second-order models of BSP and BCP.

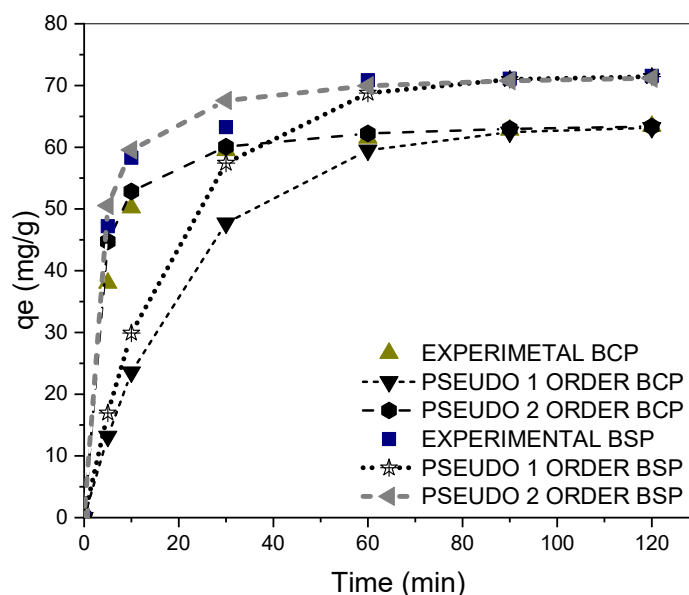| Model	Parameters	BCP	BSP
Pseudo first-order	q_e (mgg^{-1})	63.4	71.5
	k_1 (min^{-1})	0.046	0.054
	R^2	0.92	0.92
Pseudo second-order	q_e (mgg^{-1})	64.5	72.4
	k_2 (gmg^{-1}min^{-1})	0.007	0.006
	R^2	0.99	0.99

Figure 6. Comparison of experimental data with the pseudo first-order and pseudo second-order models of BSP and BCP.

Figure 7 shows the adsorption isotherms of CIP on BCP and BSP. The BSP adsorption isotherm in the study range can be classified as type L group 2c according to the Giles classification. This type of isotherm shows an adsorption on microporous materials. The initial slope shows how easy it is for solutes to find active sites; as concentration increases, the slope decreases because it is more difficult to find active sites as equilibrium is reached. The isotherm that presents the adsorption of CIP on BCP is of type L subgroup 3, which is associated with meso-microporous solids and a possible multilayer adsorption, with an inflection point that shows the completion of the monolayer [49]. These results are explained by the difference in the values of the greater specific surface for BSP. BSP behaves like a microporous solid, while BCP has the characteristics of a mesoporous solid.

Figure 7 shows the fit to the Langmuir, Freundlich, and BET models. In the case of BSP adsorption, the Freundlich model fits better experimental data, indicating a heterogeneous surface and possible multilayer adsorption. The fit of this model has been reported by other researchers in the adsorption of CIP on various adsorbents [45,47]. The value for both adsorbents is greater than 1, which means favorable adsorption, although this model did not fit well the BCP adsorption. The Langmuir model suggests an adsorption capacity of 196.1 mgg^{-1} for BSP; this result is higher than that reported in the CIP adsorption on other Fe and Si pillared clays that reach a capacity of 98.2 and 74.5 mgg^{-1}, respectively [48].
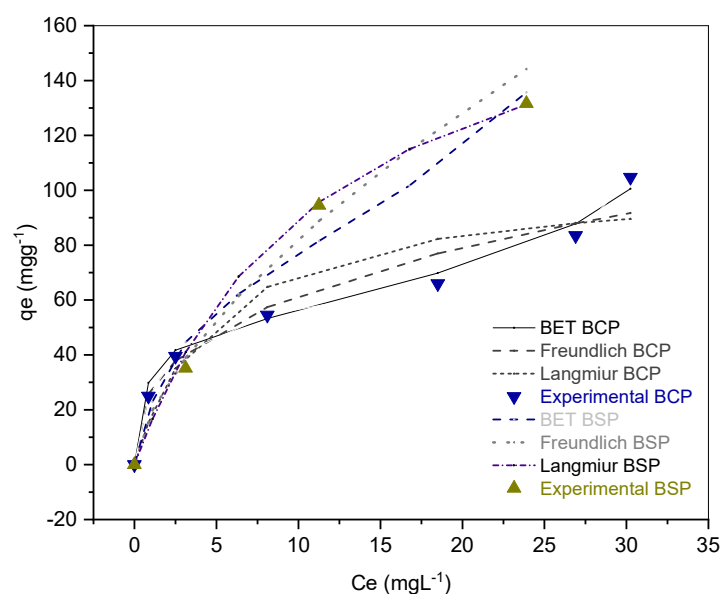
Figure 7. The adsorption isotherms of CIP on BCP and BSP, and equilibrium adsorption data of CIP and their fit to the three models: Langmuir, Freundlich and BET.

The R^2 values obtained in the linearization of the models shown in Table 5 suggest that the BET model better fits the BCP adsorption isotherm, which suggests that multilayer adsorption improves with increasing CIP solution concentration. BET model assumes that once a molecule is adsorbed, it acts as a new adsorber site. This result was also observed in the adsorption of CIP on organic residues that are macro and mesoporous materials [42].

Table 5. Parameters of the models Langmuir, Freundlich, and BET.

Model	Parameters	BCP	BSP
Langmuir	q_m (mgg^{-1})	106.4	196.1
	k_L (Lmg^{-1})	0.189	0.084
	R^2	0.91	0.97
Freundlich	k_F (mgg^{-1})	27.7	18.7
	N (gmg^{-1}min^{-1})	2.77	1.55
	R^2	0.96	0.98
BET	C_S (mgL^{-1})	58.1	49.5
	C_{BET} (Lmg^{-1})	100.2	18.6
	q_s (mgg^{-1})	50.1	78.2
	R^2	0.99	0.93
	q_d (mgg^{-1})	106.5	230.1
	k_{ad} (mol^{2}kJ^{-2})	0.0064	0.013
	E (kJmol^{-1})	8.3	6.17
	R^2	0.95	0.97

The adjustment to the Dubinin–Raduskevich (D–R) model can determine if physical or chemical adsorption occurs as a function of the value of the mean adsorption energy (E). The model indicates that the adsorption is fixed if E < 8 kJmol^{-1}, ionic exchange values are between 8 and 16 kJmol^{-1} and chemical adsorption have values greater than 16 kJmol^{-1} [46,49]. The values of E for the adsorption of CIP on BSP is less than 8 kJmol^{-1}, indicating a physical adsorption that can be given by the physical forces of Van del Waals that occur due to the aromatic rings and the hydrogen bonds formed by the F and the NH groups of the CIP with the functional groups of the adsorbent. The E value for adsorption on BCP is close to 8 kJmol^{-1}, which implies that ion exchange is not the main adsorption process.

The adsorption capacity of CIP followed the order BSP > BCP. This result could be explained by the higher specific surface of BSP. CIP is a sparingly soluble solid, therefore it adsorbs better on hydrophobic adsorbates. On the other hand, pillaring prevents the swelling of clays by increasing their hydrophobicity [45,50,51], so the hydrophobicity of pillared bentonites improves CIP adsorption. The fluoride molecule contained in the CIP acts as an acceptor of the electrons present in the pillared clays. The pillaring with Ti improves the acidic properties due to the electro-positivity of Ti. π–π interactions and Van der Waals forces are also responsible for CIP adsorption.

4. Conclusions

Pillarization improves the absorption of bentonites by increasing the surface area available for the adsorption of molecules and by increasing the stability of the clay structure. The pillaring of natural clays with titanium tetraisopropoxide improved the adsorption characteristic; the results show that the surface areas had a significant increase, especially in sodium bentonite. The kinetic studies demonstrated that adsorption reached equilibrium at 60 min, showing fast adsorption compared to other adsorbents used to remove CIP. The best fit to the adsorption kinetics was obtained with a pseudo second-order model. The adsorption isotherms show that the pillared bentonites have a high adsorption capacity of CIP. The isotherms are type L, which indicates a high affinity of mesoporous and microporous materials with the adsorbate (CIP). The maximum adsorption capacity is 196.1 mg/g reached when using BSP. This study favors the projection of the use of local clays as adsorbents for drugs in contaminated water.

References

1.　Davis, R.; Markham, A.; Balfour, J.A. Ciprofloxacin: An Updated Review of its Pharmacology, Therapeutic Efficacy and Tolerability. *Drugs* **1996**, *51*, 1019–1074. [CrossRef] [PubMed]

2.　Azriouil, M.; Aghris, S.; Matrouf, M.; Loudiki, A.; Laghrib, F.; Farahi, A.; Bakasse, M.; Saqrane, S.; Lahrich, S.; El Mhammedi, M.A. Efficacy of clay materials for ciprofloxacin antibiotic analysis in urine and pharmaceutical products. *Mater. Chem. Phys.* **2022**, *279*, 125787. [CrossRef]

3.　Chin, K.W.; Michelle Tiong, H.L.; Luang-In, V.; Ma, N.L. An overview of antibiotic and antibiotic resistance. *Environ. Adv.* **2023**, *11*, 100331. [CrossRef]

4.　Zheng, D.; Wu, M.; Zheng, E.; Wang, Y.; Feng, C.; Zou, J.; Juan, M.; Bai, X.; Wang, T.; Shi, Y. Adsorption and oxidation of ciprofloxacin by a novel layered double hydroxides modified sludge biochar. *J. Colloid Interface Sci.* **2022**, *625*, 596–605. [CrossRef] [PubMed]

5.　Microbial Polyethylene Terephthalate Hydrolases: Current and Future Perspectives-PubMed. Available online: https://pubmed.ncbi.nlm.nih.gov/33262744/ (accessed on 20 February 2022).

6.　Awad, A.M.; Shaikh, S.M.R.; Jalab, R.; Gulied, M.H.; Nasser, M.S.; Benamor, A.; Adham, S. Adsorption of organic pollutants by natural and modified clays: A comprehensive review. *Sep. Purif. Technol.* **2019**, *228*, 115719. [CrossRef]

7.　Kutuzova, A.; Dontsova, T.; Kwapinski, W. Application of TiO$_2$-Based Photocatalysts to Antibiotics Degradation: Cases of Sulfamethoxazole, Trimethoprim and Ciprofloxacin. *Catalysts* **2021**, *11*, 728. [CrossRef]

8.　Kürekci, C.; Aydın, M.; Tekeli, İ.O.; Ambarcıoğlu, P.; Şengül, S.A.; Sakin, F. Occurrence and characterization of ciprofloxacin-resistant *Escherichia Coli* from bovine and ovine bulk tank milk samples in Turkey. *J. Food Saf.* **2021**, *41*, e12881. [CrossRef]

9.　Vélez, V.P.P.; Esquivel-Hernández, G.; Cipriani-Avila, I.; Mora-Abril, E.; Cisneros, J.F.; Alvarado, A.; Abril-Ulloa, V. Emerging Contaminants in Trans-American Waters. *Rev. Ambient. Água* **2019**, *14*, 1. [CrossRef]

10.　Ashfaq, M.; Khan, K.N.; Rasool, S.; Mustafa, G.; Saif-Ur-Rehman, M.; Nazar, M.F.; Sun, Q.; Yu, C.-P. Occurrence and ecological risk assessment of fluoroquinolone antibiotics in hospital waste of Lahore, Pakistan. *Environ. Toxicol. Pharmacol.* **2016**, *42*, 16–22. [CrossRef]

11. Loos, R.; Carvalho, R.; António, D.C.; Comero, S.; Locoro, G.; Tavazzi, S.; Paracchini, B.; Ghiani, M.; Lettieri, T.; Blaha, L.; et al. EU-wide monitoring survey on emerging polar organic contaminants in wastewater treatment plant effluents. *Water Res.* **2013**, *47*, 6475–6487. [CrossRef]

12. Alderton, I.; Palmer, B.R.; Heinemann, J.A.; Pattis, I.; Weaver, L.; Gutiérrez-Ginés, M.J.; Horswell, J.; Tremblay, L.A. The role of emerging organic contaminants in the development of antimicrobial resistance. *Emerg. Contam.* **2021**, *7*, 160–171. [CrossRef]

13. Martins, A.F.; Vasconcelos, T.G.; Henriques, D.M.; Frank, C.D.S.; König, A.; Kümmerer, K. Concentration of Ciprofloxacin in Brazilian Hospital Effluent and Preliminary Risk Assessment: A Case Study. *CLEAN Soil Air Water* **2008**, *36*, 264–269. [CrossRef]

14. Igwegbe, C.A.; Oba, S.N.; Aniagor, C.O.; Adeniyi, A.G.; Ighalo, J.O. Adsorption of ciprofloxacin from water: A comprehensive review. *J. Ind. Eng. Chem.* **2021**, *93*, 57–77. [CrossRef]

15. Arcentales-Ríos, R.; Carrión-Méndez, A.; Cipriani-Ávila, I.; Acosta, S.; Capparelli, M.; Moulatlet, G.M.; Pinos-Vélez, V. Assessment of metals, emerging contaminants, and physicochemical characteristics in the drinking water and wastewater of Cuenca, Ecuador. *J. Trace Elem. Miner.* **2022**, *2*, 100030. [CrossRef]

16. Pérez-González, A.; Pinos-Vélez, V.; Cipriani-Avila, I.; Capparelli, M.; Jara-Negrete, E.; Alvarado, A.; Cisneros, J.F.; Tripaldi, P. Adsorption of Estradiol by Natural Clays and Daphnia magna as Biological Filter in an Aqueous Mixture with Emerging Contaminants. *Eng* **2021**, *2*, 312–324. [CrossRef]

17. Antunes, M.; Esteves, V.I.; Guégan, R.; Crespo, J.S.; Fernandes, A.N.; Giovanela, M. Removal of diclofenac sodium from aqueous solution by Isabel grape bagasse. *Chem. Eng. J.* **2012**, *192*, 114–121. [CrossRef]

18. Dhiman, N. Analysis of non competitive and competitive adsorption behaviour of ciprofloxacin hydrochloride and ofloxacin hydrochloride from aqueous solution using oryza sativa husk ash (single and binary adsorption of antibiotics). *Clean. Mater.* **2022**, *5*, 100108. [CrossRef]

19. Luo, H.; Ni, C.; Zhang, C.; Wang, W.; Yang, Y.; Xiong, W.; Cheng, M.; Zhou, C.; Zhou, Y.; Tian, S.; et al. Lignocellulosic biomass derived N-doped and CoO-loaded carbocatalyst used as highly efficient peroxymonosulfate activator for ciprofloxacin degradation. *J. Colloid Interface Sci.* **2022**, *610*, 221–233. [CrossRef]

20. Nguyen, T.-K.-T.; Nguyen, T.-B.; Chen, W.-H.; Chen, C.-W.; Kumar Patel, A.; Bui, X.-T.; Chen, L.; Singhania, R.R.; Dong, C.-D. Phosphoric acid-activated biochar derived from sunflower seed husk: Selective antibiotic adsorption behavior and mechanism. *Bioresour. Technol.* **2023**, *371*, 128593. [CrossRef]

21. Tong, F.; Liu, D.; Zhang, Z.; Chen, W.; Fan, G.; Gao, Y.; Gu, X.; Gu, C. Heavy metal-mediated adsorption of antibiotic tetracycline and ciprofloxacin on two microplastics: Insights into the role of complexation. *Environ. Res.* **2023**, *216*, 114716. [CrossRef]

22. Ewis, D.; Ba-Abbad, M.M.; Benamor, A.; El-Naas, M.H. Adsorption of organic water pollutants by clays and clay minerals composites: A comprehensive review. *Appl. Clay Sci.* **2022**, *229*, 106686. [CrossRef]

23. Yang, H.; Cui, Y.; Han, T.; Sandström, L.; Jönsson, P.; Yang, W. High-purity syngas production by cascaded catalytic reforming of biomass pyrolysis vapors. *Appl. Energy* **2022**, *322*, 119501. [CrossRef]

24. Ross, C.S.; Shannon, E.V. The Minerals of Bentonite and Related Clays and Their Physical Properties1. *J. Am. Ceram. Soc.* **1926**, *9*, 77–96. [CrossRef]

25. Genç, N.; Dogan, E.C. Adsorption kinetics of the antibiotic ciprofloxacin on bentonite, activated carbon, zeolite, and pumice. *Desalin. Water Treat.* **2015**, *53*, 785–793. [CrossRef]

26. Schoonheydt, R.A.; Pinnavaia, T.; Lagaly, G.; Gangas, N. Pillared Clays and Pillared Layered Solids. *Pure Appl. Chem.* **1999**, *71*, 2367–2371. [CrossRef]

27. Gil, A.; Korili, S.A.; Trujillano, R.; Vicente, M.A. A review on characterization of pillared clays by specific techniques. *Appl. Clay Sci.* **2011**, *53*, 97–105. [CrossRef]

28. Hou, M.-F.; Ma, C.-X.; Zhang, W.-D.; Tang, X.-Y.; Fan, Y.-N.; Wan, H.-F. Removal of rhodamine B using iron-pillared bentonite. *J. Hazard. Mater.* **2011**, *186*, 1118–1123. [CrossRef]

29. Şahin, Ö.; Kaya, M.; Saka, C. Plasma-surface modification on bentonite clay to improve the performance of adsorption of methylene blue. *Appl. Clay Sci.* **2015**, *116–117*, 46–53. [CrossRef]

30. Roca Jalil, M.; Baschini, M.; Sapag, K. Removal of Ciprofloxacin from Aqueous Solutions Using Pillared Clays. *Materials* **2017**, *10*, 1345. [CrossRef]

31. Chauhan, M.; Saini, V.K.; Suthar, S. Ti-pillared montmorillonite clay for adsorptive removal of amoxicillin, imipramine, diclofenac-sodium, and paracetamol from water. *J. Hazard. Mater.* **2020**, *399*, 122832. [CrossRef]

32. Hamza, W.; Chtara, C.; Benzina, M. Characterization and application of Fe and iso-Ti-pillared bentonite on retention of organic matter contained in wet industrial phosphoric acid (54%): Kinetic study. *Res. Chem. Intermed.* **2015**, *41*, 6117–6140. [CrossRef]

33. Desai, H.; Kannan, A.; Reddy, G.S.K. Sustainable and rapid pillared clay synthesis with applications in removal of anionic and cationic dyes. *Microporous Mesoporous Mater.* **2023**, *352*, 112488. [CrossRef]

34. Díez, E.; Redondo, C.; Gómez, J.M.; Miranda, R.; Rodríguez, A. Zeolite Adsorbents for Selective Removal of Co(II) and Li(I) from Aqueous Solutions. *Water* **2023**, *15*, 270. [CrossRef]

35. Yuh-Shan, H. Citation review of Lagergren kinetic rate equation on adsorption reactions. *Scientometrics* **2004**, *59*, 171–177. [CrossRef]

36. Ho, Y.S.; McKay, G. Pseudo-second order model for sorption processes. *Process Biochem.* **1999**, *34*, 451–465. [CrossRef]

37. Foo, K.Y.; Hameed, B.H. Insights into the modeling of adsorption isotherm systems. *Chem. Eng. J.* **2010**, *156*, 2–10. [CrossRef]

38. Ebadi, A.; Soltan Mohammadzadeh, J.S.; Khudiev, A. What is the correct form of BET isotherm for modeling liquid phase adsorption? *Adsorption* **2009**, *15*, 65–73. [CrossRef]

39. Liao, P.; Zhan, Z.; Dai, J.; Wu, X.; Zhang, W.; Wang, K.; Yuan, S. Adsorption of tetracycline and chloramphenicol in aqueous solutions by bamboo charcoal: A batch and fixed-bed column study. *Chem. Eng. J.* **2013**, *228*, 496–505. [CrossRef]

40. Farajfaed, S.; Sharifian, S.; Asasian-Kolur, N.; Sillanpää, M. Granular silica pillared clay for levofloxacin and gemifloxacin adsorption from aqueous systems. *J. Environ. Chem. Eng.* **2021**, *9*, 106306. [CrossRef]

41. Ojima, J. Determining of Crystalline Silica in Respirable Dust Samples by Infrared Spectrophotometry in the Presence of Interferences. *J. Occup. Health* **2003**, *45*, 94–103. [CrossRef]

42. Peñafiel, M.E.; Matesanz, J.M.; Vanegas, E.; Bermejo, D.; Mosteo, R.; Ormad, M.P. Comparative adsorption of ciprofloxacin on sugarcane bagasse from Ecuador and on commercial powdered activated carbon. *Sci. Total Environ.* **2021**, *750*, 141498. [CrossRef]

43. Zhang, B.; Han, X.; Gu, P.; Fang, S.; Bai, J. Response surface methodology approach for optimization of ciprofloxacin adsorption using activated carbon derived from the residue of desilicated rice husk. *J. Mol. Liq.* **2017**, *238*, 316–325. [CrossRef]

44. Khokhar, T.S.; Memon, F.N.; Memon, A.A.; Durmaz, F.; Memon, S.; Panhwar, Q.K.; Muneer, S. Removal of ciprofloxacin from aqueous solution using wheat bran as adsorbent. *Sep. Sci. Technol.* **2019**, *54*, 1278–1288. [CrossRef]

45. Peng, X.; Hu, F.; Huang, J.; Wang, Y.; Dai, H.; Liu, Z. Preparation of a graphitic ordered mesoporous carbon and its application in sorption of ciprofloxacin: Kinetics, isotherm, adsorption mechanisms studies. *Microporous Mesoporous Mater.* **2016**, *228*, 196–206. [CrossRef]

46. Yu, F.; Sun, Y.; Yang, M.; Ma, J. Adsorption mechanism and effect of moisture contents on ciprofloxacin removal by three-dimensional porous graphene hydrogel. *J. Hazard. Mater.* **2019**, *374*, 195–202. [CrossRef] [PubMed]

47. Turk Sekulic, M.; Boskovic, N.; Slavkovic, A.; Garunovic, J.; Kolakovic, S.; Pap, S. Surface functionalised adsorbent for emerging pharmaceutical removal: Adsorption performance and mechanisms. *Process Saf. Environ. Prot.* **2019**, *125*, 50–63. [CrossRef]

48. Maggio, A.A.; Jalil, M.E.R.; Villarroel-Rocha, J.; Sapag, K.; Baschini, M.T. Fe- and SiFe-pillared clays from a mineralogical waste as adsorbents of ciprofloxacin from water. *Appl. Clay Sci.* **2022**, *220*, 106458. [CrossRef]

49. Giles, C.H.; Smith, D.; Huitson, A. A general treatment and classification of the solute adsorption isotherm. I. Theoretical. *J. Colloid Interface Sci.* **1974**, *47*, 755–765. [CrossRef]

50. Chen, H.; Gao, B.; Li, H. Removal of sulfamethoxazole and ciprofloxacin from aqueous solutions by graphene oxide. *J. Hazard. Mater.* **2015**, *282*, 201–207. [CrossRef] [PubMed]

51. Helfferich, F.G. *Ion Exchange in Dover Science Books*; Dover ed.; Dover Publications: New York, NY, USA, 1995; ISBN 978-0-486-68784-1.